Low-energy quantum dynamics of atoms at defects. Interstitial oxygen in silicon

Rafael Ramírez,[1] Carlos P. Herrero,[1] Emilio Artacho,[2] and Félix Ynduráin[2]
[1] *Instituto de Ciencia de Materiales, Consejo Superior de Investigaciones Científicas (C.S.I.C.), Campus de Cantoblanco, 28049 Madrid, Spain*
[2] *Instituto de Ciencia de Materiales Nicolás Cabrera and Departamento de Física de la Materia Condensada, C-III, Universidad Autónoma de Madrid, 28049 Madrid, Spain*
(15 July 1996)

The problem of the low-energy highly-anharmonic quantum dynamics of isolated impurities in solids is addressed by using path-integral Monte Carlo simulations. Interstitial oxygen in silicon is studied as a prototypical example showing such a behavior. The assignment of a "geometry" to the defect is discussed. Depending on the potential (or on the impurity mass), there is a "classical" regime, where the maximum probability-density for the oxygen nucleus is at the potential minimum. There is another regime, associated to highly anharmonic potentials, where this is not the case. Both regimes are separated by a sharp transition. Also, the decoupling of the many-nuclei problem into a one-body Hamiltonian to describe the low-energy dynamics is studied. The adiabatic potential obtained from the relaxation of all the other degrees of freedom at each value of the coordinate associated to the low-energy motion, gives the best approximation to the full many-nuclei problem.

arXiv:cond-mat/9607115v4 30 Jul 1996

I. INTRODUCTION

The dynamics of impurities or, more generally, atoms at point defects in crystalline solids quite often gives rise to localized low-energy excitations, typically in the far infrared (FIR) spectral region, displaying patterns that reflect, in one way or another, a substantial deviation from the situation of atomic nuclei harmonically vibrating around their potential minimum.[1–3] For example, interstitial H or Li around other substitutional impurities in Si and Ge are delocalized among several positions equivalent by symmetry, giving rise to FIR excitations.[4] Similar FIR excitation patterns are found in glasses.[5] Mixed crystals have recently been shown to exhibit a similar behavior.[6]

The substantial deviation from harmonicity in these systems, considering the quantum character of their dynamics, is of great importance in their characterization. On one hand, the quantum character prevents the assignment of a definite geometry to the defect structure, the nuclei showing high probability for being found away from the potential minimum location. On the other hand, the anharmonicity makes that the many-nuclei problem cannot be easily decoupled as usually in terms of normal modes of vibration, leaving open the question of what is the best decoupling approximation, that accounts for the experimental observations of those low-energy excitations.

Interstitial oxygen (O_i) in silicon also displays nontrivial quantum behavior.[1,7,8] The oxygen atom is known to break a Si–Si bond, establishing two Si–O bonds in the form of an oxygen bridge. The motion of the oxygen atom and its neighbors in the direction of the axis of the original Si–Si bond can be described in terms of harmonic vibrations, which account for some of the main features in the infrared absorption spectrum of the center.[8] It is the motion of the oxygen atom in the plane perpendicular to that axis what gives rise to the non-trivial behavior, characterized by a peculiar FIR spectrum.[1] The symmetry of the center corresponds to the D_{3d} point group. This symmetry facilitates the a priori partial decoupling of the relevant degrees of freedom. It is this fact, together with the availability of experimental and theoretical information, what makes this system particularly suitable for analysis of the questions raised above: (i) can we define a geometry for the center, and (ii) what is the best way of decoupling the low-energy dynamics from the rest.

The relevance of the geometry question has already been pointed out in the literature.[8] It was observed that, for the effective potential obtained from experiment,[7] the oxygen atom has maximum probability-density at the bond-center (BC) site in spite of being the potential a local maximum at that point. The arguments used there, however, are for the effective one-particle Hamiltonian, and have to be checked for the fully interacting problem.

The importance of the decoupling problem is clear by the analysis of the experimental FIR spectra in terms of finding an effective one-particle potential in two dimensions, such that an oxygen atom moving under that potential would reproduce the vibrational frequencies observed in the spectra. It is an axially-symmetric potential well with a local maximum at the bond-center and a minimum around it, at 0.22 Å off the BC site (mexican-hat shape).[7] The energy barrier amounts to ≈ 1 meV. If we consider the fact that the oxygen atom is strongly interacting with its silicon neighbors, the question arises: what is the meaning of that potential? The multidimensional potential associated to all the nuclear degrees of freedom of the system is well defined, but not a two-dimensional one, unless a decoupling prescription is available. In similar situations, when the harmonic decoupling is meaningless, propositions for decoupling are found in the literature ranging between two extremes. Arguing on the basis of the lightness of the impurity atom, some

authors[9] propose that the effective one-particle potential for the motion of that impurity is the one obtained when the host (heavier) atoms are kept fixed at some defined positions (fixed-lattice potential; FLP, hereafter): the effective slower motion of the host atoms is presumed from mass considerations. The other extreme can be also stated in terms of the different times scales of the relative motions, but taking now into consideration the energies associated to those motions. In this latter case it is the impurity (or some of its degrees of freedom) the slow moving, in spite of its lightness. This argument leads to an adiabatic potential (AP) that is obtained by allowing the host atoms to relax for each value of the coordinates associated to the low-energy degrees of freedom.

These questions are addressed in this paper by solving the full quantum many-nuclei problem of interstitial oxygen in silicon by means of path-integral (PI) Monte Carlo (MC) simulations. This paper is divided up in the following manner. In Sec. II we briefly describe the computational method and summarize the details concerning the potential used. Sec. III is devoted to the results and discussion. The geometry of the center O_i is assessed with the probability-density function of the oxygen nucleus. The decoupling of the low-energy motion is studied by comparing the results of the complete MC simulations with those derived according to different decoupling criteria. The paper closes with a summary (Sec. IV).

II. COMPUTATIONAL METHOD

A. Path-integral simulations

The PI MC method has become a standard tool to study finite-temperature properties of quantum systems. In this Section we briefly present the details relevant for the presentation of our results. More complete descriptions of the PI formalism can be found elsewhere.[12–16] The canonical partition function of P silicon nuclei plus the O impurity can be expressed with the Trotter formula and the high-temperature approximation for the density matrix[13] as:

$$Z \approx \left(\frac{m_{\rm O}}{m_{\rm Si}}\right)^{3N/2} \left(\frac{N m_{\rm Si}}{2\pi\beta\hbar^2}\right)^{3(P+1)N/2} \int \prod_{j=1}^{N} d\mathbf{R}_j \ \exp\left\{-\beta v_{\rm eff}(\mathbf{R}_1, ..., \mathbf{R}_N)\right\} . \tag{1}$$

The index j represents the path coordinate along a cyclic path, which has been decomposed into a number N of discrete intervals (Trotter number). $\mathbf{R}_j$ is a vector in a $3(P+1)$-dimensional space, whose components are the Cartesian coordinates of the $P+1$ nuclei $(\mathbf{r}_{1,j}; ...; \mathbf{r}_{P+1,j})$. The cyclic condition for the path coordinate of each nucleus is expressed as $\mathbf{R}_{N+1} = \mathbf{R}_1$. The masses of the host and impurity atoms are $m_{\rm Si}$ and $m_{\rm O}$, respectively; $\beta = (k_B T)^{-1}$, and k_B is the Boltzmann constant. Eq. (1) coincides with the canonical partition function of a classical system with the effective interaction potential:

$$v_{\rm eff}(\mathbf{R}_1, ..., \mathbf{R}_N) = \sum_{j=1}^{N} \left\{ A(\mathbf{R}_j, \mathbf{R}_{j+1}) + N^{-1} V(\mathbf{R}_j) \right\} , \tag{2}$$

where

$$A(\mathbf{R}_j, \mathbf{R}_{j+1}) = \frac{N}{2\beta^2\hbar^2} \left\{ m_{\rm O} (\mathbf{r}_{P+1,j+1} - \mathbf{r}_{P+1,j})^2 + \sum_{p=1}^{P} m_{\rm Si} (\mathbf{r}_{p,j+1} - \mathbf{r}_{pj})^2 \right\} . \tag{3}$$

The index p indicates the particle, and goes from 1 to P for the silicon atoms, and takes the value $P+1$ for the impurity. The function $v_{\rm eff}(\mathbf{R}_1, ..., \mathbf{R}_N)$ is the interaction potential of a classical system composed of $P+1$ cyclic chains [one per nucleus; a total of $N(P+1)$ classical particles] characterized by a harmonic intrachain coupling with a force constant $\kappa = mN/\beta^2\hbar^2$ [first term on the right-hand side of Eq. (2); $m = m_{\rm Si}$ or $m_{\rm O}$, depending on the nucleus]. Interchain coupling [second term on the right-hand side of Eq. (2)] is restricted to those particles with the same index j, and this interaction is equal to that corresponding to the quantum particles, $V(\mathbf{R}_j)$, but renormalized by a factor N^{-1} (inverse of the number of discrete points along the path coordinate). The approximated expression for Z [Eq. (1)] becomes exact in the limit $N \to \infty$, and is valid for distinguishable particles. This assumption of distinguishable particles is reasonable for the statistics of Si nuclei, since exchange effects are negligible.

Equilibrium properties of the quantum system can be derived by Metropolis Monte Carlo sampling of the multidimensional integral associated to the partition function given by Eq. (1).[17–19] A simulation run proceeds via successive MC steps (MCS). In each MCS, the nuclei coordinates $\mathbf{r}_{p,j}$ are updated according to two different kinds of sampling

schemes. The first one consists on trial moves of the individual coordinates $\mathbf{r}_{p,j}$. The trials are performed sequentially for every path coordinate j and every nucleus p. The second type of sampling] corresponds to trial moves of the center of gravity of the cyclic paths, that are carried out sequentially for every nucleus p in the simulation cell. The number of MCS's employed for system equilibration was of 5×10^3, while the calculation of ensemble average properties was performed over 2×10^5 MCS's. For the Si atoms we have employed the average isotope mass of this element ($m = 28.086$ amu). The number N of discretized points for the path coordinate was made temperature dependent, and was taken as the integral number closest to $2000/T$, a condition that guarantees convergence in the total energy within a relative error smaller than 1%.[20]

B. Potential

The Monte Carlo simulations have been performed on a $2 \times 2 \times 2$ supercell of the Si face-centered cubic (fcc) cell containing 64 Si atoms and an oxygen impurity. The simulation cell was subject to periodic boundary conditions. The interaction between silicon atoms has been described by the three-body potential developed by Stillinger and Weber.[10] The potential between oxygen and silicon atoms has been designed to reproduce qualitatively the main features of the O_i defect: (i) the overall geometry, O breaking a bond between two Si atoms; (ii) the observed low-energy (FIR) excitations[1] (even though the PI does not provide excited states, it does give internal energy versus temperature, which, at low temperatures is mainly controlled by these low-energy excitations); (iii) the vibrations of the center at higher frequencies, known by infrared absorption;[11] and (iv) the main features of the potential obtained from first-principles calculations, including bond lengths, bond angle, and Si relaxations.[8] This potential for the interaction between O and Si atoms is a function of the coordinates of both the impurity ($\mathbf{r}_{\rm O}$), and the Si atoms ($\mathbf{r}_1$ and $\mathbf{r}_2$) coordinated to the oxygen:

$$V(\mathbf{r}_1, \mathbf{r}_2, \mathbf{r}_{\rm O}) = V_r(r_{1\rm O}) + V_r(r_{2\rm O}) + V_s(\alpha) + V_l(\alpha) \ , \quad (4)$$

where $\mathbf{r}_{i\rm O} = \mathbf{r}_i - \mathbf{r}_{\rm O}$ (i =1, 2), and α is the angle Si–O–Si. The potential functions are:

$$V_r(r) = \frac{1}{2} k (r - r_e)^2 \ , \quad (5)$$

$$V_s(\alpha) = s_1 \sin^2 \alpha + s_2 \sin^4 \alpha \ , \quad (6)$$

$$V_l(\alpha) = l_1 (\cos \alpha - \cos \alpha_e)^2 \ , \quad (7)$$

with the following values of the constants: $k = 35.6$ eV Å^{-2}, $r_e = 1.629$ Å, $s_1 = 1.49$ eV, $s_2 = -0.7484$ eV, $l_1 = 5.4$ eV, and $\alpha_e = 168^{\rm o}$. The local geometry of the defect complex is shown in Fig. 1. The absolute potential minimum corresponds to a geometry with the oxygen nucleus located at the off-center position M, at a distance of about 0.29 Å from the Si–Si axis. The corresponding Si–O distance is 1.52 Å and the Si–O–Si angle is 158$^{\rm o}$. The relaxation of the nearest Si atoms along the [111] crystal direction amounts to 0.32 Å. For comparison, the Si–O distance obtained from total-energy Hartree-Fock calculations[8] of the O_i defect is 1.56 Å, with an outwards relaxation of the nearest Si atoms of 0.36 Å each. The vibrational frequency of the A_{1g} mode at the O_i center derived from our model potential is 587 cm^{-1}, while the frequency reported in a cluster-Bethe-lattice investigation[8] of the O_i defect was 569 cm^{-1}. This mode corresponds to atom displacements along the Si–Si axis and has no infrared activity because of symmetry. The potential energy for the impurity located at the BC site is higher than that found for the absolute minimum. This value agrees with that of ~ 1 meV corresponding to the model potential of Yamada-Kaneta *et al.*,[7] which was designed to reproduce the spectrum of low-energy excitations of the O_i center. When the oxygen is located at the BC site, our parametrized potential gives a relaxation of the nearest Si atoms of 0.35 Å.

In Fig. 2(a), a calculated potential energy surface is presented as a function of both the distance between the Si atoms nearest neighbors of O, d(Si–Si), and the distance from the oxygen atom to the bond-center site as oxygen moves in the plane perpendicular to the Si–Si axis, d(O–BC). For every point in the figure, the positions of the other Si atoms were relaxed. The curves obtained by sectioning the surface for fixed values of d(Si–Si) correspond to FLP's. For distances d(Si–Si) larger than 3.04 Å the minimum energy is found when the oxygen atom is located at the BC site. However, at smaller values of d(Si–Si), the minimum is found for an off-center position. In Fig. 2(b) we present two sections of the energy surface calculated at representative distances d(Si–Si). The broken line shows the FLP derived with the Si atoms fixed at their relaxed positions for the absolute minimum of the potential, the oxygen impurity being located at the off-center position M, with d(Si–Si) = 3 Å (called FLP-1, hereafter). The energy barrier amounts to $\sim$ 24 meV. The solid line corresponds to a fixed-lattice potential (FLP-2) with the hosts atoms fixed at their relaxed positions for the O nucleus located at the BC site and $d(\rm Si_1–Si_2) = 3.05$ Å. The dotted line connecting the minima of both curves represents the adiabatic potential (AP) characterized by an energy barrier.

III. RESULTS AND DISCUSSION

A. Geometry

In order to define a geometry for the O_i defect, we have studied the probability-density $\rho(r)$ of finding the oxygen

nucleus at a distance r from the Si–Si axis along any direction by PI MC simulations at 10 K. The full quantum treatment included the O nucleus and the nearest and next-nearest Si neighbors (i.e., a total of nine atoms), while the remaining Si atoms in the simulation cell were fixed at their relaxed positions obtained for the system at the absolute potential minimum. The probability-density $\rho(r)$ was normalized so that:

$$\int_0^\infty dr\ 2\pi r\rho(r) = 1. \tag{8}$$

In Fig. 3 the density $\rho(r)$ for the oxygen nucleus is shown by a full line. The maximum probability-density is found at the BC site, i.e., it does not correspond to the absolute minimum of the potential energy at the off-center site M. This peculiar behavior was already observed in a previous investigation assuming an effective one-particle potential for the impurity.[8] The relevance of our calculation is that this nontrivial quantum delocalization of oxygen is confirmed by a quantum approach for the full many-body potential. One expects that an impurity with larger mass, interacting through the same potential as that employed for oxygen, will approach a "classical" behavior, in the sense that those spatial regions with larger probability-density will correspond to regions of lower potential energy. In Fig. 3, the function $\rho(r)$ obtained by setting in the PI simulation the impurity mass $m_O = 60$ amu, is displayed by a broken line. The maximum probability-density is found in this case at an off-center position. We have performed a series of simulations at 10 K varying the impurity mass in the range $m_O = 16$–150 amu. In Fig. 3(b), the position of the maximum of the $\rho(r)$ curves is presented as a function of the impurity mass m_O. For a mass larger than about 50 amu we find a "classical" regime, where the position of the maximum of $\rho(r)$ is off-center.

We note that the assignment of a definite geometry to the O_i defect is difficult and may be meaningless, because the probability-density function is very broad in the plane perpendicular to the Si–Si axis. This large spatial uncertainty is due to the zero-point motion of the impurity and therefore it cannot be reduced by decreasing the temperature. From the point of view of a structure with minimum potential energy, which is the one usually adopted in total-energy investigations using electronic structure methods, the defect geometry would correspond to a non-linear arrangement of the oxygen and the nearest-neighbor Si atoms. This is of no physical significance, however, since the maximum probability-density (and the symmetry) is for a linear disposition of the atoms. It is the highly anharmonic situation found for oxygen in silicon that leads to contradictory pictures concerning the defect geometry. This point could be relevant also for some crystalline phases, like β–cristobalite, where different structural models have been proposed, and some controversy has arisen concerning the existence of linear Si–O–Si units in this structure.[21,22]

B. Decoupling into a one-particle problem

The results derived from the full quantum mechanical treatment of the O_i defect can be used to test the quality of several alternatives (FLP versus AP) for the decoupling of the many-nuclei degrees-of-freedom into a one-body potential. In Fig. 4(a), the "exact" probability-density $\rho(r)$ for the oxygen nucleus obtained by the full PI simulation at 10 K is represented by open squares and is compared to the curves derived by four different decoupling schemes. We have analyzed three different fixed-lattice potentials FLP and the adiabatic potential AP. For each one of these potentials we have performed a one-particle PI simulation to obtain $\rho(r)$ at 10 K. The broken line in Fig. 4(a) is the result derived from the potential FLP-2, defined with the Si atoms fixed at the relaxed positions obtained with the O impurity located at the BC site. The maximum probability-density is found at the BC site in agreement with the result obtained for the full potential. However, the probability-density away from the BC site decays too fast and the curvature of the $\rho(r)$ curve does not compare well with the result of the full PI simulation. The dashed-dotted line corresponds to the potential FLP-1, defined with the Si atoms fixed at the relaxed positions obtained with the O impurity located at the off-center site M. This potential FLP-1 leads to an even more unrealistic probability-density, as the maximum density is found close to the off-center position M. The dotted line in Fig. 4(a) was derived from the third choice of a FLP, where the Si atoms were fixed at their equilibrium positions obtained from the MC trajectory generated by the full quantum simulation of the O impurity and the Si atoms. This potential FLP-3 gives a better agreement with the full simulation. However, in spite of its much larger computational requirements (it needs the results of the full quantum treatment), the improvement is still unsatisfactory. This and the other FLP approaches discussed above are not able to reproduce closely the density distribution of the impurity. At last, we present in Fig. 4(a) the results found for the oxygen impurity moving in the adiabatic potential defined in the plane perpendicular to the Si–Si axis [dotted line in Fig. 2(b)]. This $\rho(r)$ curve is shown by a full line and agrees closely with that derived by the full quantum simulation. We conclude that the best decoupling scheme for the O_i defect, in the plane perpendicular to the Si–Si axis, corresponds to the AP approximation.

It is interesting to test whether the AP potential is also able to reproduce the results of the full simulation shown in Fig. 3(b), by a series of one-body simulations for different impurity masses. The results obtained in these PI MC simulations for the position of the maximum of $\rho(r)$ are given in Fig. 4(b). The agreement with the data of the full quantum simulations of Fig. 3(b) is good. In particular, the crossover between impurity-mass ranges with maximum probability-density at BC or off-center, lies at about 50 amu, as found in the full quantum problem.

As the mass of the impurity increases, its motion with respect to the host atoms will become relatively slower, therefore the adiabatic potential remains a good approximation to the many-body problem.

Finally, we compare in Tab. I some spectroscopic information, obtained by solving numerically the two-dimensional Schrödinger equation of an oxygen nucleus moving in the AP and FLP-1 potentials, with available experimental data.[1] The frequencies derived from the AP potential show a closer agreement to the experimental results than the frequencies calculated with the FLP-1 potential. The AP transitions are about 40 % larger than those derived from experiment. However, the renormalization of the transitions to the value of the first excitation reduces this discrepancy to 12 %. This deviation from experiment can be due either to limitations in the adiabatic approximation or to shortcomings in the employed potential model. The main conclusion from the data in Tab. I is that the adiabatic potential appears again as a better decoupling approach to the full many-nuclei problem than the fixed lattice potential.

IV. CONCLUSIONS

The definition of a defect geometry for an isolated oxygen impurity in silicon is conditioned by a substantial deviation from harmonicity, as the configuration with minimum potential energy does not correspond to a maximum in the probability-density function of the oxygen nucleus. The minimum energy configuration is found for a bent Si–O–Si configuration. However, the probability-density function of the impurity, as derived by PI MC simulations, displays the symmetry of a linear arrangement of atoms. This is a case in which the structure associated to the minimum energy is not the best choice to derive some physical properties of the defect complex. The anharmonicity of the zero-point motion of the impurity and the lattice atoms reduces the importance of the minimum-energy structure for defining the properties of the impurity center.

An important property of the O_i center is that the dynamics in the plane perpendicular to the Si–Si axis is characterized by frequencies of about 30 cm^{-1}. These extremely low frequencies, even for a relatively light impurity as oxygen, cause that the best decoupling scheme for the reduction of the full many-body problem into a one-body treatment is given by the adiabatic potential, where for each impurity position the Si atoms (moving faster) relax to their equilibrium sites.

Low-energy excitations are normally associated to localized defect states. Some of the physics, however, is very much related to other dynamical phenomena like diffusion. Specifically, the problem of the delocalization of light impurity atoms among symmetry-equivalent sites around another atom[4] is essentially the same as what is found for the diffusion of those light atoms, where the delocalization is among sites equivalent by translational symmetry. The discussion in this paper about the definition of a static defect structure is partially transferable to the dynamical problem of defining diffusion paths for quantum particles.

ACKNOWLEDGMENTS

We thank Pedro L. de Andrés for critical comments on the manuscript. This work was supported by DGICYT (Spain) under contracts PB93-1254 and PB92-0169.

[1] W. Hayes and D. R. Bosomworth, Phys. Rev. Lett. **23**, 851 (1969); D. R. Bosomworth, W. Hayes, A. R. L. Spray, and G. D. Watkins, Proc. Roy. Soc. Lond. A **317**, 133 (1970).
[2] M. Gienger, M. Glaser, and K. Laßmann, Solid State Commun. **86**, 285 (1993).
[3] K. Muro and A. J. Sievers, Phys. Rev. Lett. **57**, 897 (1986).
[4] See E. Artacho and L. M. Falicov, Phys. Rev. B **43**, 12507 (1991), and references therein for the (H,Be) complex in Si, and E. E. Haller and L. M. Falicov, Phys. Rev. Lett. **41**, 1192 (1978), for the (Li,O) complex in Ge.
[5] M.A. Bösch, Phys. Rev. Lett. **40**, 879 (1978), and references therein.
[6] S. A. Fitzgerald, J. A. Campbell, and A. J. Sievers, Phys. Rev. Lett. **73**, 3105 (1994).
[7] H. Yamada-Kaneta, C. Kaneta, and T. Ogawa, Phys. Rev. B **42**, 9650 (1990).
[8] E. Artacho, A. Lizón-Nordström, and F. Ynduráin, Phys. Rev. B **51**, 7862 (1995).
[9] P. J. H. Denteneer, C. G. Van de Walle, and S. T. Pantelides, Phys. Rev. Lett. **62**, 1884 (1989).
[10] F.H. Stillinger and T.A. Weber, Phys. Rev. B **31**, 5262 (1985).
[11] B. Pajot, E. Artacho, C. A. J. Amerlaan, and J. M. Spaeth, J. Phys.: Condens. Matter **7**, 7077 (1995) and references therein.
[12] D.M. Ceperley, Rev. Mod. Phys. **62**, 279 (1995).
[13] M.J. Gillan in *Computer Modelling of Fluids, Polymers, and Solids*, edited by C.R.A. Catlow, S.C. Parker, and M.P. Allen (Kluwer, Dordrecht, 1990); M.J. Gillan, Phil. Mag. A **58**, 257 (1988).
[14] M. Takahashi and M. Imada, J. Phys. Soc. Jpn. **53**, 963 (1984); **53**, 3765 (1984).
[15] D.L. Freeman and J.D. Doll, J. Chem. Phys. **80**, 5709 (1984).
[16] E.L. Pollock and D.M. Ceperley, Phys. Rev B **30**, 2555 (1984).
[17] N. Metropolis, A.W. Rosenbluth, M.N. Rosenbluth, A.H. Teller, and E. Teller, J. Chem. Phys. **21**, 1087 (1953).
[18] J.P. Valleau in *Computer Simulation in Materials Science*, edited by M. Meyer and V. Pontikis (Kluwer, Dordrecht, 1991).

[19] K. Binder and D.W. Heermann, *Monte Carlo Simulation in Statistical Physics* (Springer, Berlin, 1988).
[20] R. Ramírez and C.P. Herrero, Phys. Rev. B **48**, 14659 (1993).
[21] F. Liu, S.H. Garofalini, R.D. King-Smith, and D. Vanderbilt, Phys. Rev. Lett. **70**, 2750 (1993).
[22] I.P. Swainson and M.T. Dove, Phys. Rev. Lett. **71**, 193 (1993).

FIG. 1. Schematic representation of the atom disposition in the O_i center. Alternative sites for the oxygen nucleus are indicated by BC (bond-center) and M (off-center). The absolute minimum of the employed potential model corresponds to the off-center site M, 0.29 Å away from the BC site.

FIG. 2. (a) Potential energy for the nuclear motion shown versus the O distance to the BC site within the plane perpendicular to the Si–Si axis, and versus the Si–Si distance between host atoms nearest-neighbors of O. The contour interval is 3 meV. (b) Three different one-dimensional cuts are presented: (i) for the Si atoms fixed at the positions of the absolute potential-minimum (fixed-lattice potential FLP-1, broken line); (ii) for the Si atoms fixed at their relaxed positions for O at the BC site (FLP-2, full line) , and (iii) for the Si atoms relaxing at each O position (adiabatic potential, AP, dotted line). (i) and (ii) are cuts of the potential surface in (a), in vertical planes parallel to the d(O–BC) axis.

FIG. 3. (a) Probability-density $\rho(r)$ for the O nucleus obtained in the full PI simulation at 10 K. r is the distance from the impurity to the Si–Si axis. The full line corresponds to $m_{\rm O} = 16$ amu and the broken line to $m_{\rm O} = 60$ amu. (b) Distance from the probability-density maximum to the Si–Si axis, as a function of the impurity mass. The broken line is a guide to the eye.

FIG. 4. (a) Comparison of probability-density curves of the O nucleus for different one-particle potentials with that derived by the many-particle simulation (open squares). The broken, dotted, and dashed-dotted lines correspond to different FLP models (see text), while the full line is the result of the adiabatic potential (AP). (b) Position of the maximum in the probability-density $\rho(r)$ corresponding to the adiabatic potential, as a function of the impurity mass. The broken line is a guide to the eye.

TABLE I. Observed and calculated FIR transitions ($\rm cm^{-1}$) of oxygen in silicon. The calculated values correspond to the AP and FLP-1 potentials. In parenthesis are given the relative values with respect to the first transition. The observed values are taken from Ref. [1].

Transition	obs.		AP		FLP-1	
$\|0,0\rangle \rightarrow \|1,\pm1\rangle$	29.3	(1)	37.1	(1)	24.1	(1)
$\|1,\pm1\rangle \rightarrow \|2,\pm2\rangle$	37.8	(1.3)	51.6	(1.4)	51.6	(2.1)
$\|2,\pm2\rangle \rightarrow \|3,\pm3\rangle$	43.3	(1.5)	62.9	(1.7)	70.9	(2.9)
$\|1,\pm1\rangle \rightarrow \|2,0\rangle$	49.0	(1.7)	72.6	(2.0)	140.3	(5.8)

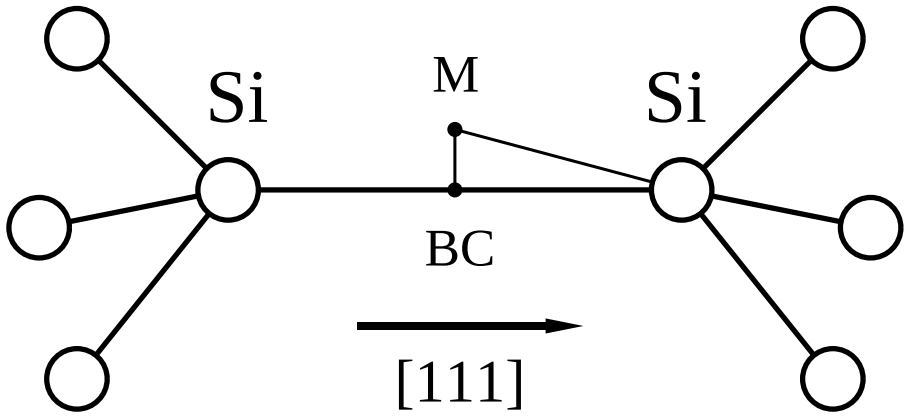
Si
M
Si
BC
[111]

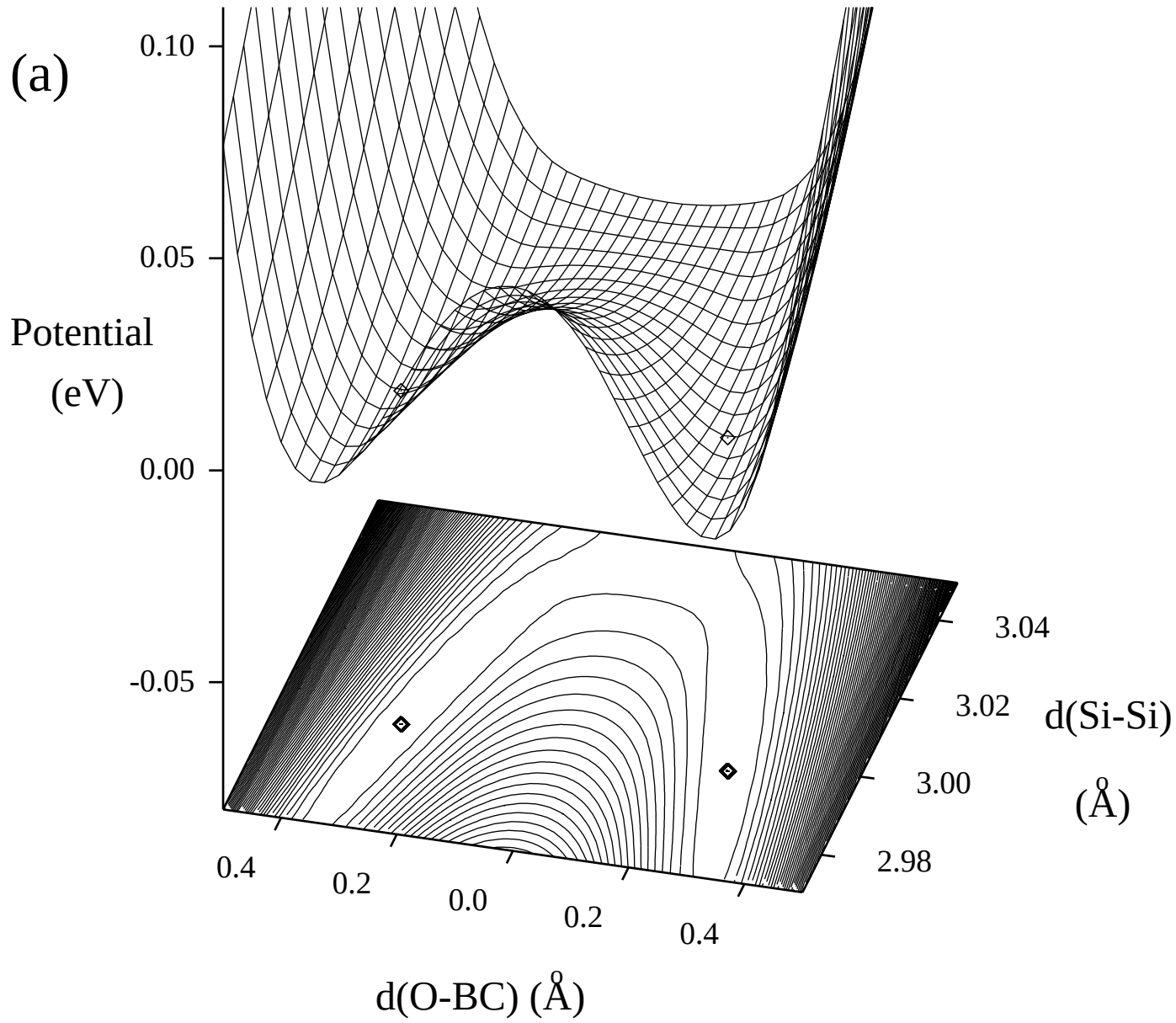
(a)
0.10
0.05
0.00
-0.05
Potential
(eV)
3.04
3.02
3.00
2.98
d(Si-Si)
(Å)
0.4
0.2
0.0
0.2
0.4
d(O-BC) (Å)

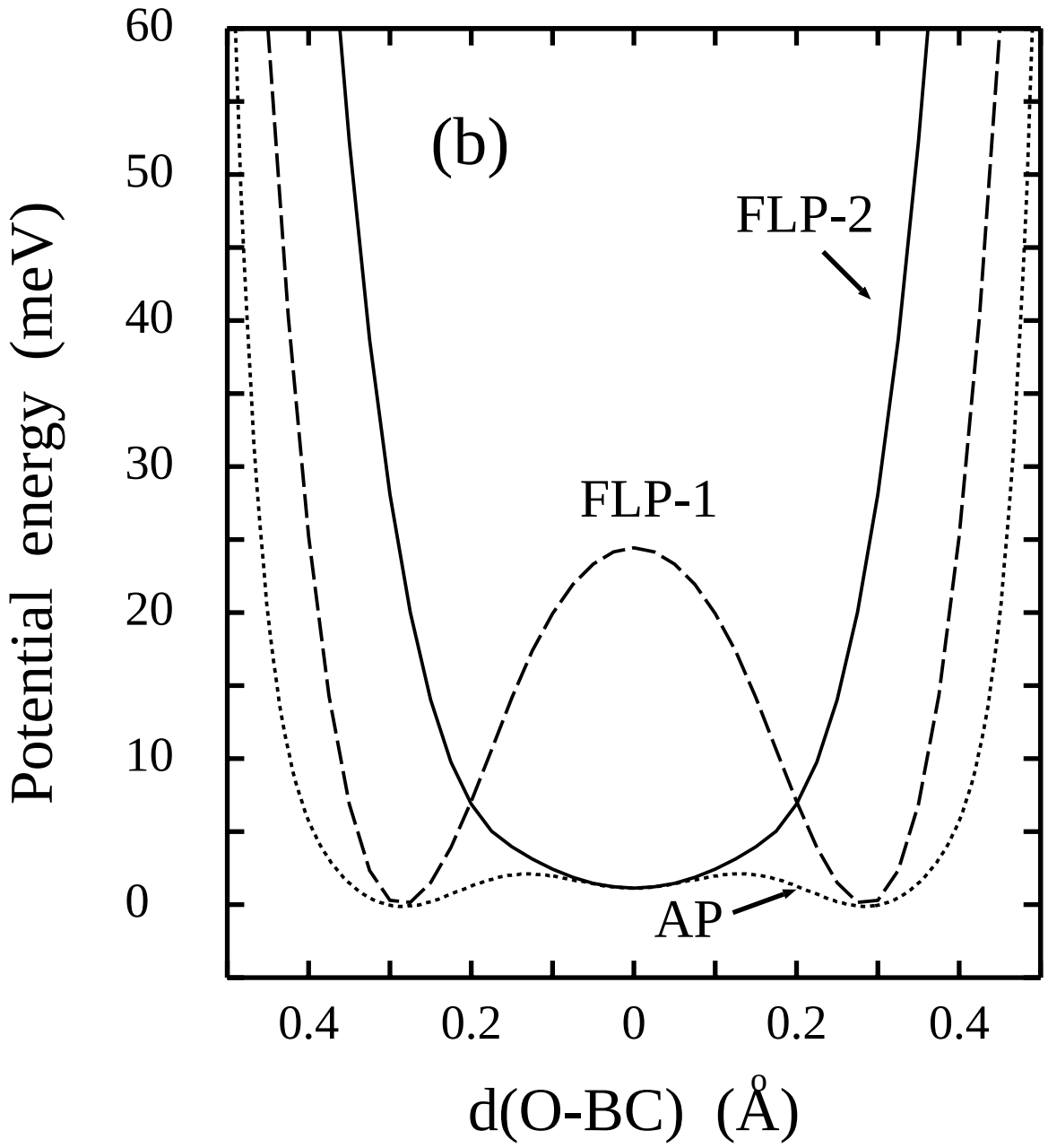
(b)
FLP-2
FLP-1
AP
Potential energy (meV)
d(O-BC) (Å)
60
50
40
30
20
10
0
0.4
0.2
0
0.2
0.4

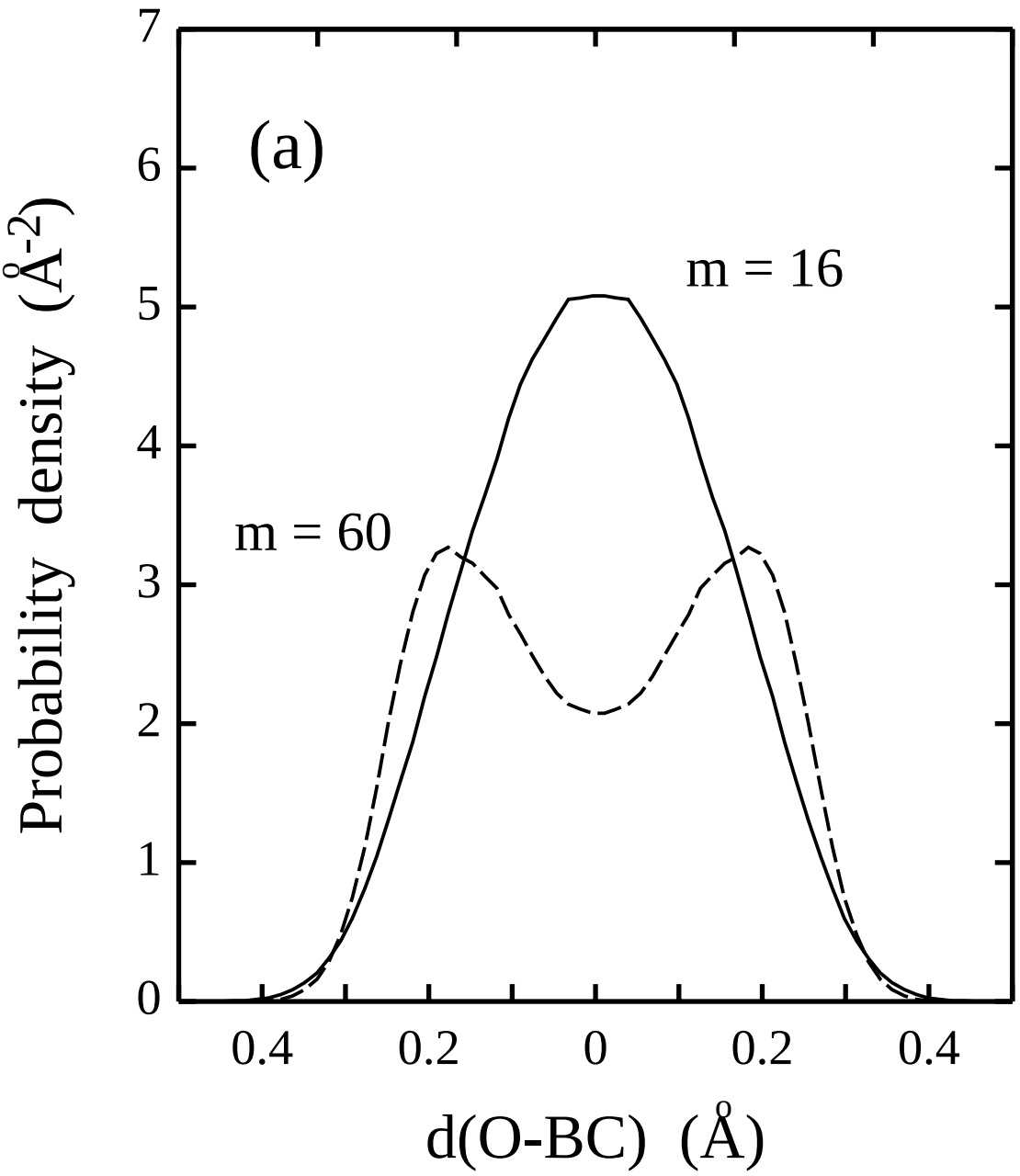
(a)
m = 16
m = 60
Probability density (Å-2)
d(O-BC) (Å)
0
1
2
3
4
5
6
7
0.4
0.2
0
0.2
0.4

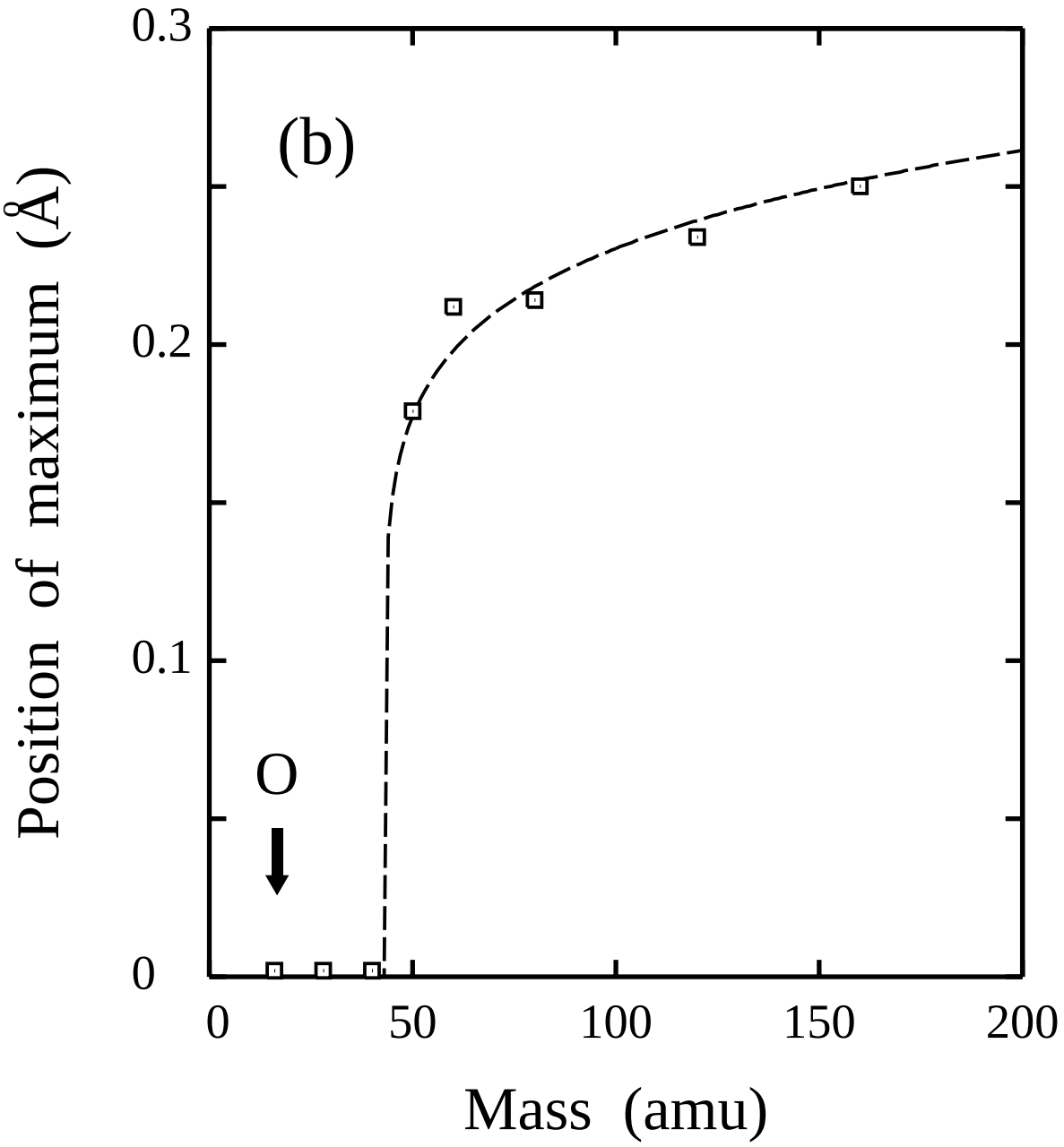
(b)
O
Position of maximum (Å)
Mass (amu)
0
0.1
0.2
0.3
0
50
100
150
200

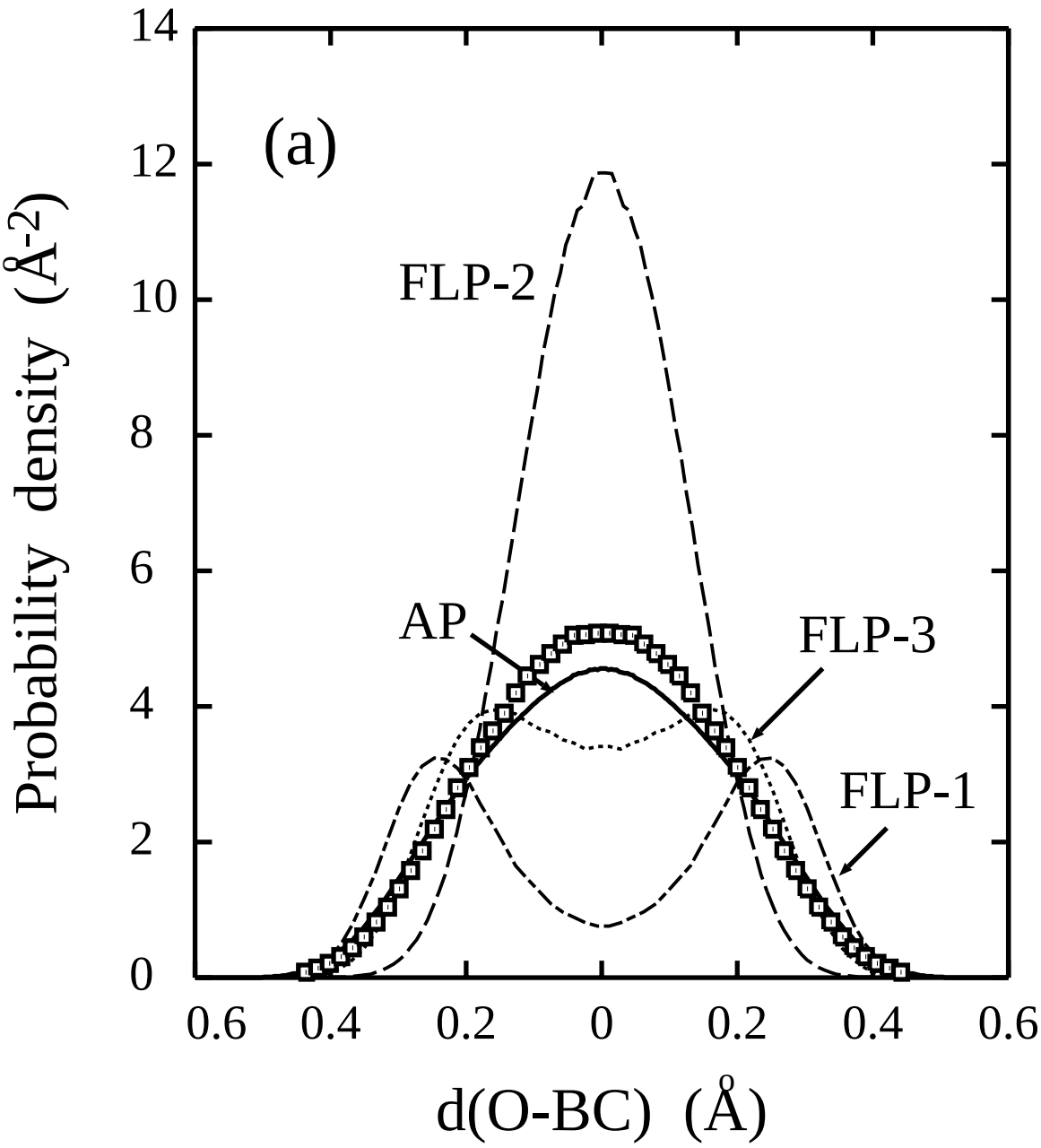
(a)
FLP-2
AP
FLP-3
FLP-1
Probability density (Å-2)
d(O-BC) (Å)
14
12
10
8
6
4
2
0
0.6
0.4
0.2
0
0.2
0.4
0.6

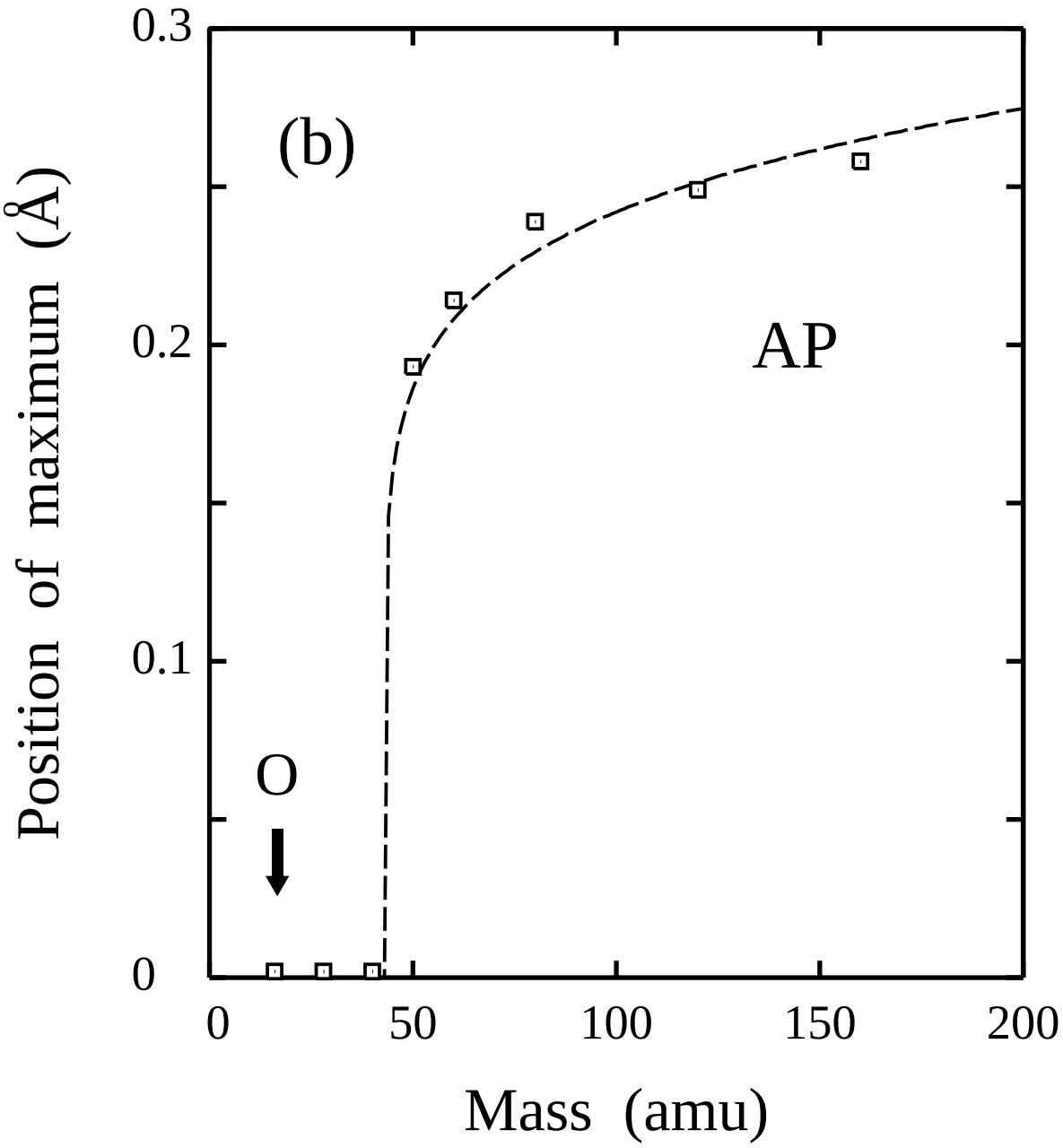
(b)
AP
O
Position of maximum (Å)
Mass (amu)
0.3
0.2
0.1
0
0
50
100
150
200